

Response to Referee #2's comments

egusphere-2024-2940 "Investigating Plant Responses to Water Stress via Plant Hydraulics Pathway" Z.Song, Y.Zeng, Y.Wang, E.Tang, D.Yu, F.Alidoost, M.Ma, X.Han, X.Tang, Z.Zhu, Y.Xiao, D.Kong, Z.Su

The article presents a very thorough investigation of an addition to the STEMMUS-SCOPE model to include the effects of plant water stress on the simulation of sub-daily soil-plant-atmosphere dynamics and transfers of mass and energy. The work needs a little reorganisation but is generally easy to read. There are several important questions to answer however that will require moderate revision to address.

We appreciate this reviewer's insightful and constructive feedback, which has significantly contributed to improving our manuscript. We have revised the manuscript accordingly.

Some of the details in the Supplementary material need to be included in the main text. For example, the fact that you ran the simulation for nearly one-year but show the results only for two particular weeks. What period do you estimate the fitting statistics over; I am assuming it is only the one week shown in each set of figures.

Thank you for your constructive suggestion. The comparison of simulated soil moisture (Fig. R1) and soil temperature (Fig. R2) will be moved to the main text in Section 3.1.

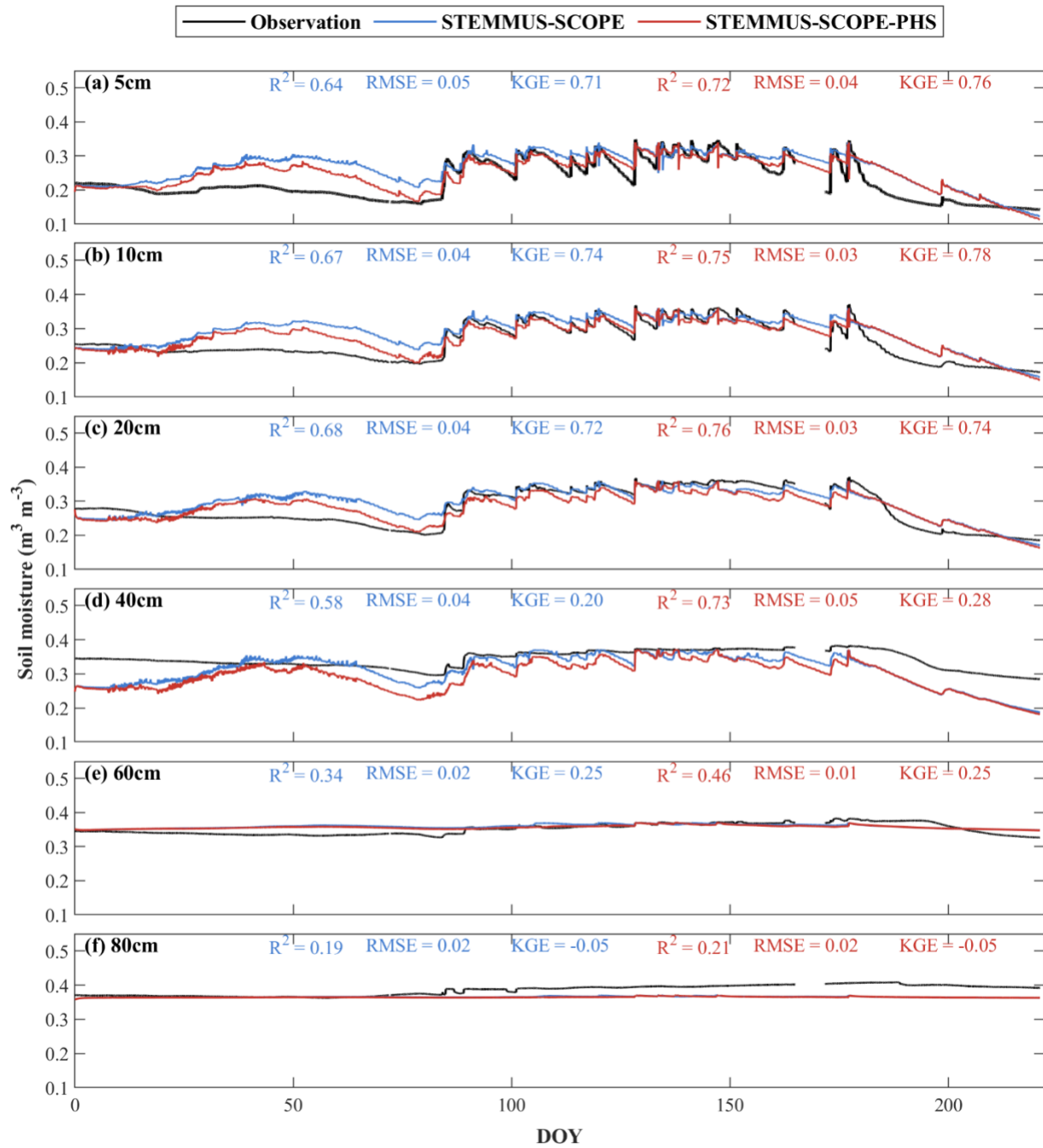


Fig. R1 Comparison of half-hourly simulated and observed soil moisture at the depth of 5, 10, 20, 40, 60 and 80 cm. The blue and red lines are the results of STEMMUS-SCOPE and STEMMUS-SCOPE-PHS, respectively.

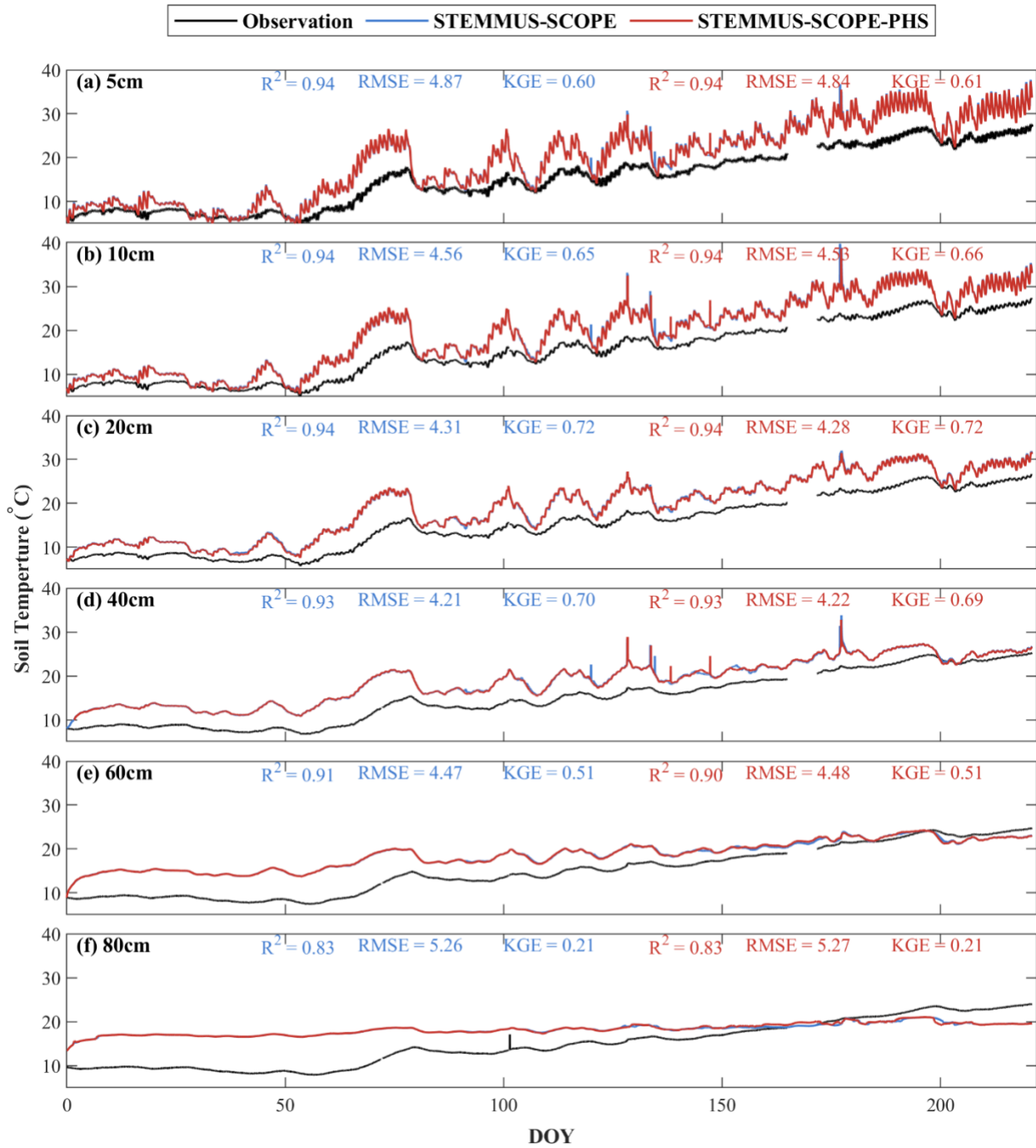


Fig. R2 Comparison of half-hourly simulated and observed soil temperature at the depth of 5, 10, 20, 40, 60 and 80 cm. The blue and red lines are the results of STEMMUS-SCOPE and STEMMUS-SOCPE-PHS, respectively.

The entire period of comparison of energy and carbon fluxes, as well as SIF and PAR are shown Figs. R3-4 (Figures 3-4 in the main text). We have revised the captions as follows:

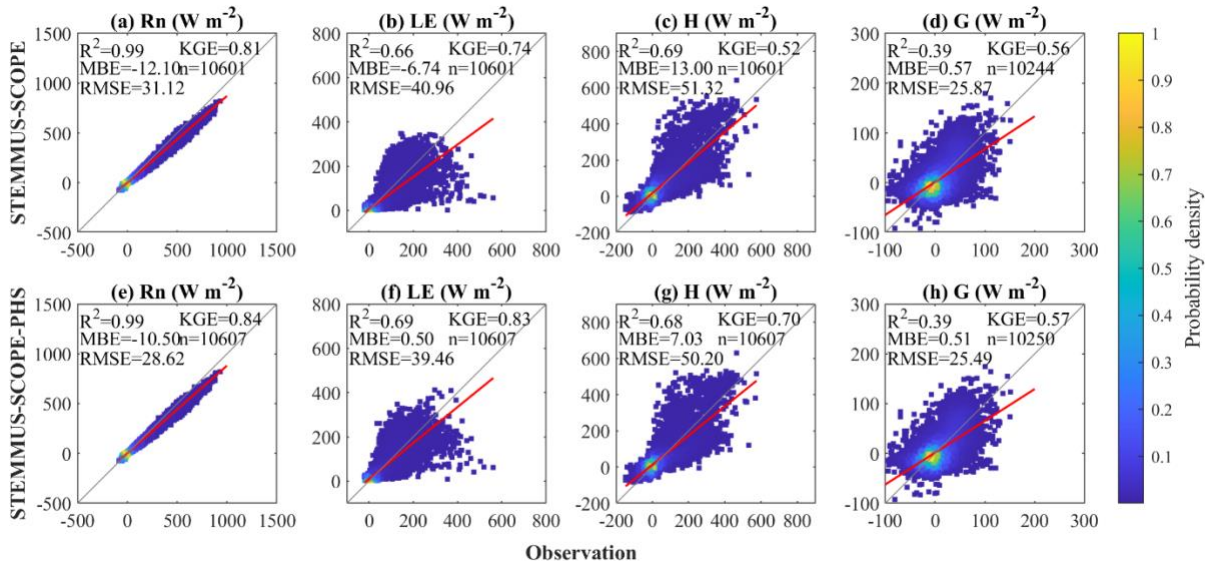


Fig. R3 Comparison of half-hourly simulated and observed net radiation (Rn) (a & e), latent heat flux (LE) (b & f), sensible heat flux (H) (c & g), and soil heat flux (G) (d & b) based on STEMMUS-SCOPE (a-d) and STEMMUS-SCOPE-PHS (e-f) from 1st January to 9th August at Hutouacun site. The x-axis represents observation, and the y-axis represents simulation. The grey line is 1:1 line, and the bold red line is the regression line. The values of R², MBE, RMSE, KGE and the numbers of points (n) are given in each subplot.

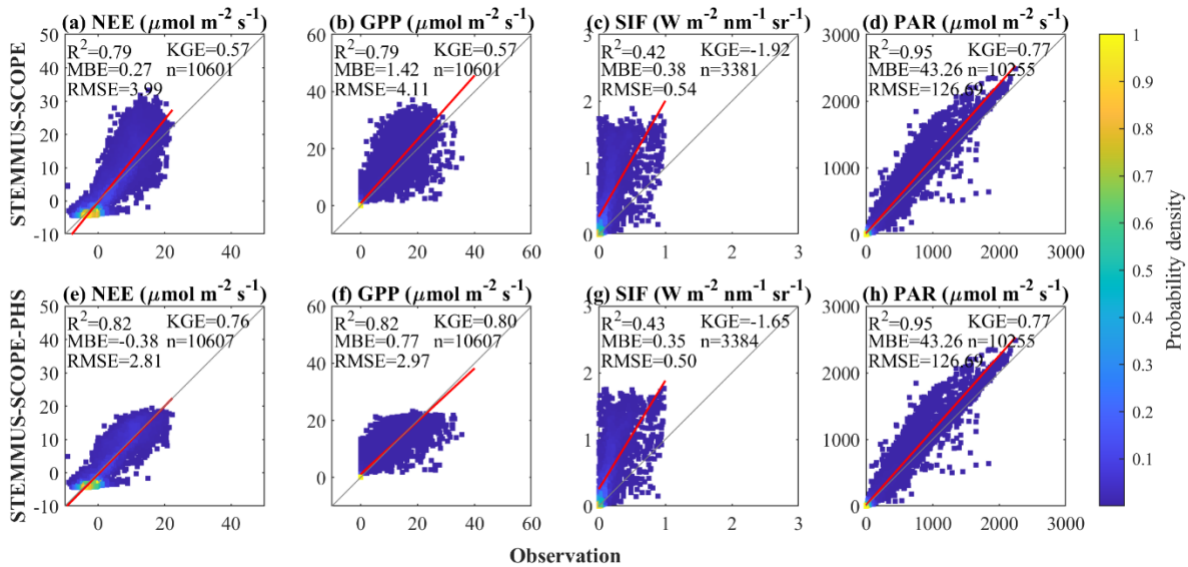


Fig. R4 Comparison of half-hourly simulated and observed net ecosystem exchange (NEE), (a & e), gross primary productivity (GPP) (b & f), solar-induced chlorophyll fluorescence (SIF) (c & g), and photosynthetically active radiation (PAR) (d & h) from 1st January to 9th August based on STEMMUS-SCOPE (a-d) and STEMMUS-SCOPE-PHS (e-h) at Hutouacun site. The x-axis represents observation, and the y-axis represents simulation. The grey line is the 1:1 line. The

bold red line is the regression line. The values of R^2 , MBE, RMSE, KGE, and the numbers of points (n) are given in each subplot.

In Figures 5-6, and Figures 8-9 in the main text, the value of R^2 , MBE, RMSE, and KGE over the entire study period (1st January to 9th August, 2022) were originally shown, as also presented in Fig. R3 and Fig. R4. Only one week of the dynamics of energy and carbon fluxes were compared between simulation and observation in each set of figures. To reduce the confusion, we have removed the statistics in these figures as:

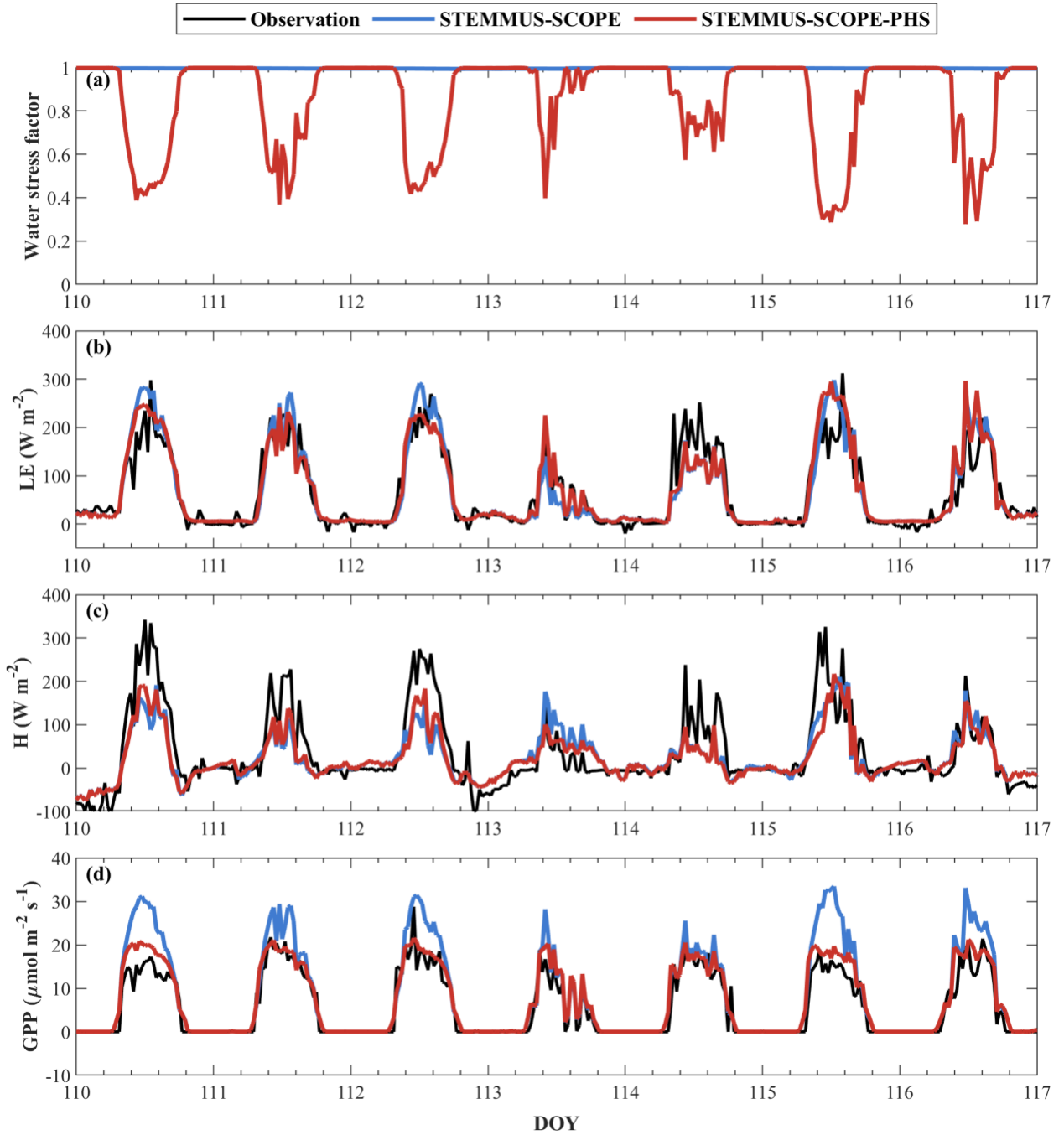


Fig. R5 Diurnal dynamics for half-hourly (a) water stress factor, (b) latent heat flux (LE , $W m^{-2}$), (c) sensible heat flux (H , $W m^{-2}$), and (d) gross primary productivity (GPP , $\mu mol m^{-2} s^{-1}$) under well-watered conditions (DOY 110-117).

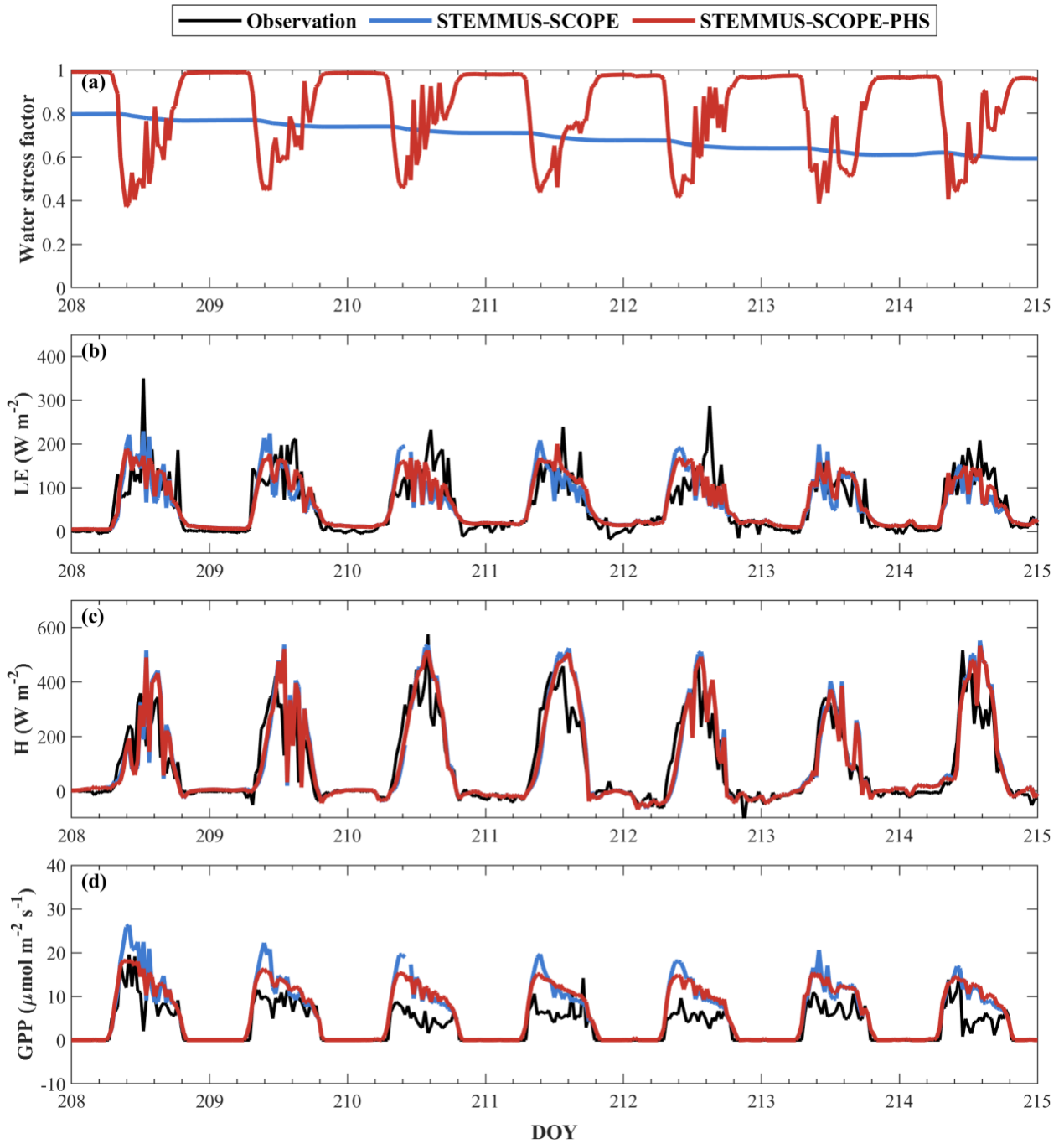


Fig. R6 Diurnal dynamics for half-hourly (a) water stress factor, (b) latent heat flux (LE , $W m^{-2}$), (c) sensible heat flux (H , $W m^{-2}$), and (d) gross primary productivity (GPP , $\mu mol m^{-2} s^{-1}$) under water-limited conditions (DOY 208-215).

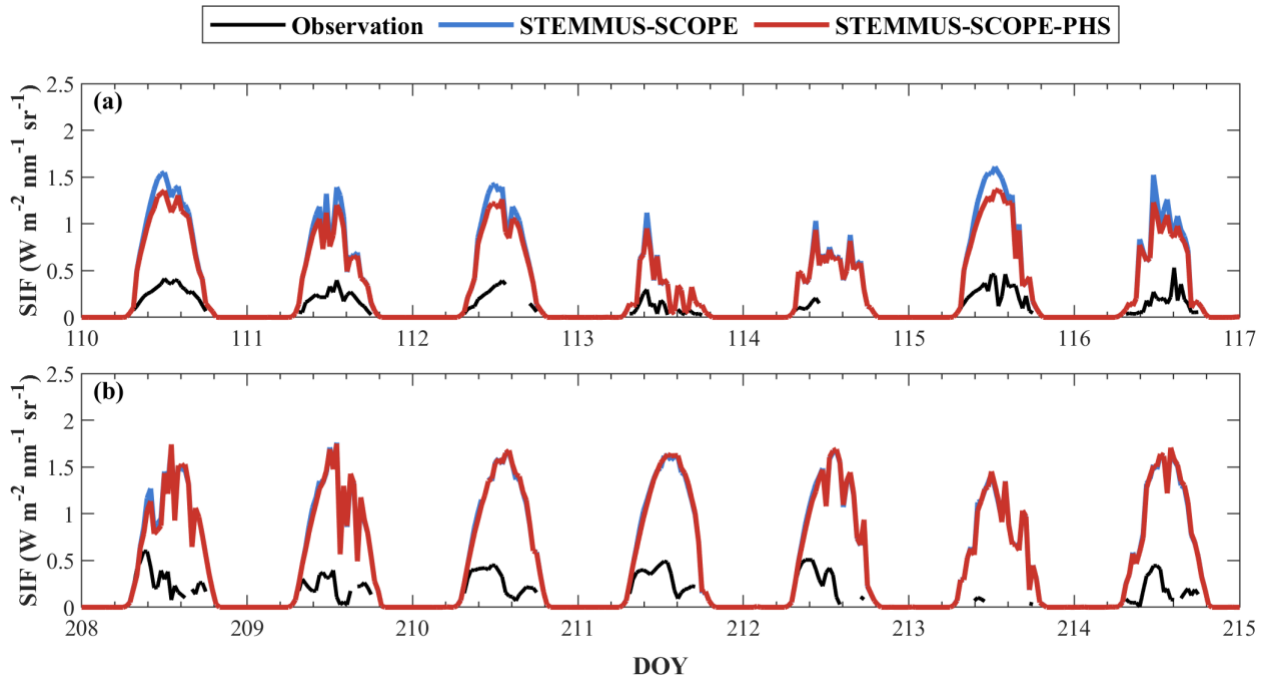


Fig. R7 Comparison of half-hourly simulated and observed SIF at 760 nm. The black line is observed SIF. The blue and red line are simulated SIF by STEMMUS-SCOPE and STEMMUS-SCOPE-PHS, respectively. (a) is well-watered condition, and (b) is water-limited condition.

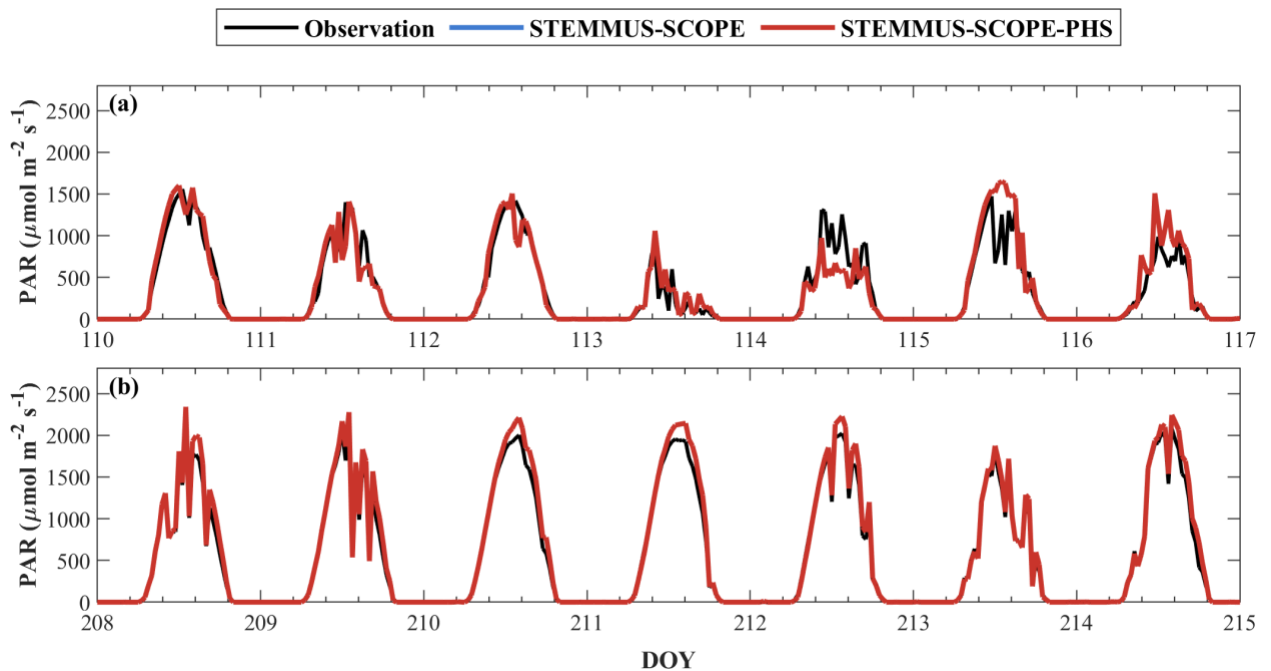


Fig. R8 Comparison of half-hourly simulated and observed PAR. The black line is observed PAR, and the blue and red line are simulated PAR by STEMMUS-SCOPE and STEMMUS-SCOPE-PHS, respectively, for which the blue and red lines overlap. (a) is well-watered condition, and (b) is water-limited condition.

Regarding the half-hourly dynamics of fluxes, pooling nearly one-year half-hourly simulation results into one figure does not tell much dynamics (Fig. R9 and Fig. R10), and we have added them into the supplementary. The shorter time series is used to understand better the comparison result between model and observation.

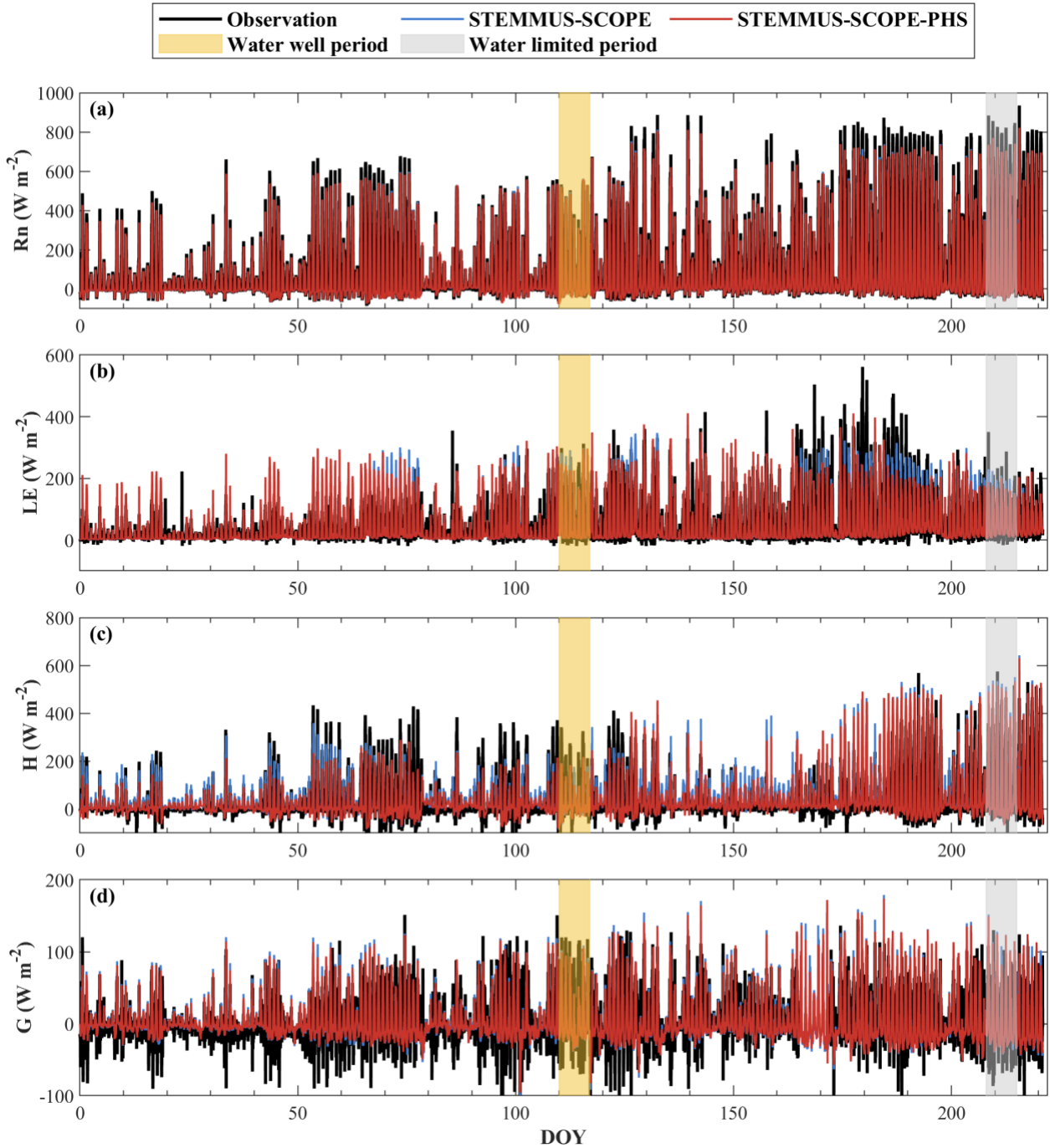


Fig. R9 Comparing of half-hourly simulated and observed net radiation (a), latent heat flux (b), sensible heat flux (c) and soil heat flux (d) from 1st January to 9th August, 2022 at the Hutoucun site. The blue and red line are the simulation from STEMMUS-SCOPE and STEMMUS-SCOPE-

PHS, respectively. The well-watered period and water-limited period are marked in yellow and grey, respectively.

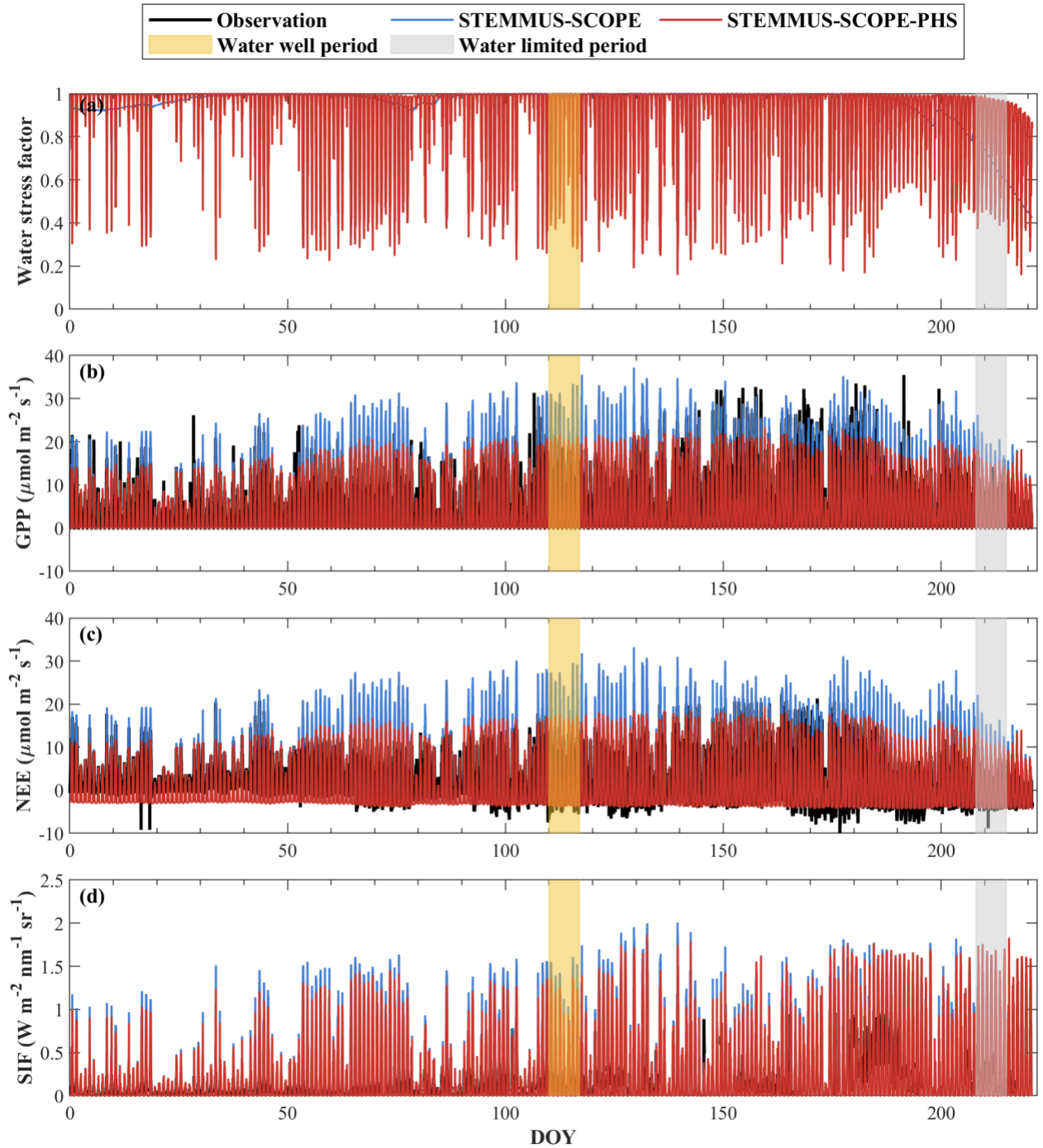


Fig. R10 Comparing of half-hourly (a) simulated water stress factor, (b) simulated and observed GPP, (c) simulated and observed NEE, (d) simulated and observed SIF from 1st January to 9th August, 2022 at the Hutouacun site. The blue and red line are the simulation from STEMMUS-SCOPE and STEMMUS-SCOPE-PHS, respectively. The water stress factors are

not observed, so only the results from two models were shown. The well-watered period and water-limited period are marked in yellow and grey, respectively.

How many soil layers were used (7) and the total depth of the soil column (1m), along with the range of time steps (1 second to 30 minutes as outlined in Zeng et al ?) should be explicit. This information can fit in a single paragraph at the end of §2.3 and allow the reader to better understand the scales involved

Regarding to the settings of simulation, the soil profile was divided into 29 layers with a total depth of 1 m. The time step of simulation was set as 30 minutes. The simulated half-hourly results were compared with half-hourly observations. The following paragraph was added as Section 2.5 to describe the model setting and validation.

2.5 Experiment Description and Model validation

2.5.1 Model Setting

In this study, the STEMMUS-SCOPE and STEMMUS-SCOPE-PHS were tested at a karst ecosystem at the Hutoucun site, Chongqing, China from 1st January to 9th August, 2022 to explore the plant response to water stress. The time step of both simulations was set as 30 minutes, the same with the temporal resolution of flux observation. The soil profile was divided into 29 layers for a total depth of 1 m. The simulated soil moisture and soil temperature at the depth of 5cm, 10 cm, 20cm, 40cm, 60cm and 80 cm were compared with in-situ observation. To better analyse the model's performance at sub-daily dynamics of carbon and energy fluxes, one week with slight dryness (Day of Year (DOY) 110-117) and one week with server dryness (DOY 208-215) were selected based on the value of soil-moisture-based water stress factor. The comparison between observations and simulations at the whole study periods were shown in Supplement (Fig. R9 and Fig. R10).

The area shown in Figure 1 indicates the flux tower is located on the northern edge of the osmanthus plantation. How does this influence the measurements given the prevailing wind direction, for example, and what is the footprint of the tower and expected fetch given the height of vegetation and the flux tower? Given the small size of the plantation, is there any limitation to using remotely-sensed data at 500m and 1000m resolutions? How many trees were instrumented to represent these data?

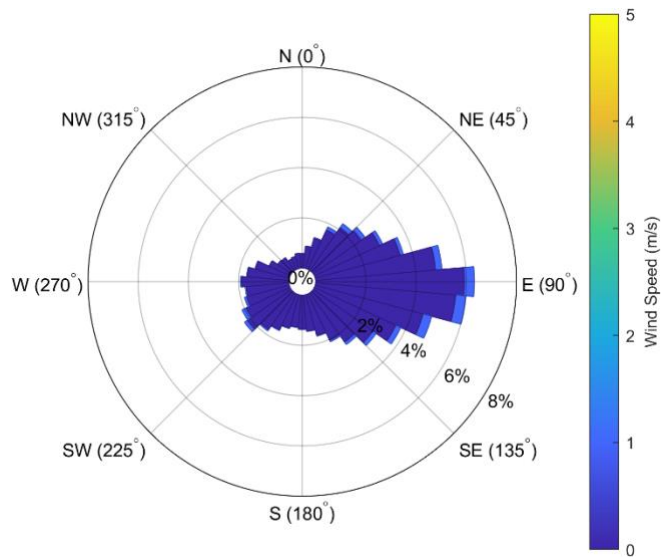


Fig. R11 Wind direction and wind speed at the Hutoucun site

Thank you for your comment. As shown in Fig. R11, the flux tower is located downwind of the main wind direction which can ensure accurate and representative measurement of the vapor and carbon fluxes. According to your comments, Fig. R11 will be added in the supplementary to show the dominant wind directions at the Hutoucun site.

At the Hutoucun site, two stem water potential sensors (PSY-1, ICT, Australia) were installed on two trees near the flux tower, one approximately 5 meters to the southeast and the other about 6 meters to the northeast.

We had added the following paragraph to discuss the impacts of using MODIS LAI at this small plantation in Section 4.1.

In STEMMUS-SCOPE-PHS, LAI was used to upscale leaf-scale latent heat flux and GPP to the canopy scale, which plays a critical role in simulating canopy and ecosystem-scale carbon and water fluxes. Bonan (1993) showed that the net carbon assimilation is highly sensitive to LAI, with uncertainties in LAI potentially introducing errors of up to 70% in simulated net carbon assimilation at forest sites. Fang et al. (2012) validated MODIS LAI products against field true LAI from 80 sites, and found that MODIS LAI agree well with field measurements in broadleaf forest. In this study, LAI was extracted from MODIS MCD15A2H.006 dataset, which has a high temporal resolution of 8 days, and a spatial resolution of 500 m. The high temporal resolution facilitates continuous monitoring of plant dynamics. However, the relatively coarse spatial resolution could lead to mixed pixel effects caused by surrounding land cover types, introducing uncertainties into model simulations. To mitigate the potential uncertainties resulting from MODIS LAI data, we calibrated it based on 5-day in-situ observation of 20 trees, and filtered it by the Harmonic Analysis of Time Series (HANTS) method (Tang et al., 2024).

The equation for SMWSF embedded in line 141 on page 5 needs to be expanded on its own line for clarity. It is not obvious what parts are in the exponential term, and I am guessing that SM(i) is the actual soil moisture in the i-th soil layer which is listed as q_i in the text.

Thank you for your comment. The SM(i) is the actual soil moisture in the i^{th} soil layer which is listed as θ_i in the text. The equation for SMWSF has been revised:

Secondly, the soil-moisture-based water stress factor at the i^{th} soil layer (SMWSF(i), Wang et al. (2021)) was calculated as a sigmoid function

$$(SMWSF(i) = \left[1 + e^{\left(-100\theta_{sat,i} \left(\theta_i - \frac{\theta_{f,i} + \theta_{w,i}}{2} \right) \right)} \right]^{-1}$$

where i represents the i^{th} soil layer. The θ_i , $\theta_{sat,i}$, $\theta_{f,i}$, and $\theta_{w,i}$ are the actual soil moisture, saturated soil moisture, field capacity, and permanent wilting point at the i^{th} soil layer, respectively.

I am confused about estimation of the transpiration flux. It is indicated in Equation (6) that it is simply energy dependent, which may be good enough in well-watered and energy-limited systems but not in general, then on the next page we are told transpiration, stomatal conductance and carbon assimilation are coupled with the Farquhar et al method. Does Equation (6) represent a potential transpiration which is then modified? How does this affect the instantly equilibrated assumption in Equation (2) and which comes first?

Thank you for your comment. Equation 6 indicates the actual transpiration (Trans) that should be suitable in all conditions. However, we have revised the draft (also according to the first reviewer's comment 1.2.1.)

$$Trans = \frac{LE_c}{m2mm \cdot \lambda}, \quad (\text{R1, eq. 6 in main text})$$

where LE_c ($W m^{-2}$) is the canopy latent heat flux, λ ($J kg^{-1}$) is the latent heat of vaporization of water. The factor $m2mm$ (=1000) converts the unit from $mm s^{-1}$ to $m s^{-1}$.

The frameworks of STEMMUS-SCOPE-PHS can be described as:

1. Transpiration

The actual canopy latent heat flux (LE_c) is calculated as (van der Tol et al., 2009):

$$LE_c = \rho_{air} \cdot \lambda \cdot \frac{q_i - q_a}{r_s + r_a}, \quad (R2)$$

where ρ_{air} (kg m^{-3}) is the specific mass of air, λ (J kg^{-1}) is the latent heat of water, $q_i(-)$ and $q_a(-)$ are intercellular and atmospheric absolute humidity, r_s (s m^{-1}) and r_a (s m^{-1}) are stomatal and aerodynamics resistance, respectively.

The transpiration is calculated by eq.R1.

2. Calculation of leaf water potential and plant water stress factor

Water balance equation:

$$\sum_{i=1}^n q_{soil-root,i} = q_{root-stem} = q_{stem-leaf} = Trans, \quad (R3)$$

where the $q_{soil-root,i}$, $q_{root-stem}$, $q_{stem-leaf}$ represent the water fluxes (m s^{-1}) from soil to roots, roots to stem, and stem to leaf, respectively. The *Trans* means transpiration (m s^{-1}). The subscript i indicates the i^{th} soil layer.

The root water potential at the i^{th} layer ($\psi_{root,i}$) is calculated as:

$$\psi_{root,i} = \psi_{soil,i} - z_i - \frac{q_{soil-root,i}}{k_{soil-root,i}}, \quad (R4)$$

where $\psi_{soil,i}$ (m) is soil water potential at the i^{th} layer, z_i (m) means the depth of i^{th} soil layer, $k_{soil-root,i}$ (s^{-1}) is soil to root hydraulic conductance.

The stem water potential is calculated as:

$$\psi_{stem} = \psi_{root} - h - \frac{q_{root-stem}}{k_{root-stem} \times SAI}, \quad (R5)$$

where h (m) is the height of the canopy that is equal to gravitational potential, $k_{root-stem}$ (s^{-1}) is hydraulic conductance from root to stem. SAI ($\text{m}^2 \text{m}^{-2}$) is stem area index.

The leaf water potential is calculated as:

$$\psi_{leaf} = \psi_{stem} - \frac{q_{stem-leaf}}{k_{stem-leaf} \times LAI}, \quad (R6)$$

where $k_{stem-leaf}$ (s^{-1}) is hydraulic conductance from stem to leaf, LAI ($\text{m}^2 \text{m}^{-2}$) is leaf area index.

Once leaf water potential is available, plant water stress can be calculated based on the scheme in ED2 model as

$$phwsf_{ED2} = \left[1 + \left(\frac{\psi_{leaf}}{P50_{leaf}} \right)^a \right]^{-1}, \quad (R7)$$

or based on the scheme in CLM as:

$$phwsf_{CLM} = 2^{-\left(\frac{\psi_{leaf}}{P50_{leaf}} \right)^{ck_{leaf}}}, \quad (R8)$$

where $P50_{leaf}$ (m) is the water potential at the 50% hydraulic conductance loss and a (or ck_{leaf}) is a shape parameter.

3. Water stress effects on photosynthesis

Carbon assimilation is calculated by (Wang et al., 2021):

$$A_n = \begin{cases} \min(V_c, V_e), & \text{for C3 plants} \\ \min(V_c, V_e, V_s), & \text{for C4 plants} \end{cases}, \quad (R9)$$

$$V_c = V_{c,max} \times phwsf, \quad (R10)$$

The $phwsf$ is the leaf water potential-based water stress factor.

4. calculation of stomatal conductance

Stomatal conductance g_s ($mol\ m^{-2}s^{-1}$) is calculated by:

$$g_s = g_0 + a_{c2w} \cdot \left(1 + \frac{g_1}{\sqrt{D}} \right) \left(\frac{A_n \cdot ppm2bar}{C_a} \right) \quad (R11)$$

where g_s is stomatal conductance ($mol\ m^{-2}s^{-1}$) for water molecule, g_0 is the minimum stomatal conductance ($mol\ m^{-2}s^{-1}$), g_1 is the slope of stomatal conductance ($hPa^{0.5}$), D is water vapor pressure deficit (hPa), C_a is the CO_2 concentration at the leaf surface (bar). The a_{c2w} equals 1.6, which is used to convert the conductance of CO_2 to that of water vapor. A_n is the net carbon assimilation rate ($\mu mol\ m^{-2}s^{-1}$), ppm2bar converts the units from $\mu mol\ mol^{-1}$ to bar.

To clarify the framework of the STEMMUS-SCOPE-PHS, a flowchart (Fig. R12) has been added accordingly.

Energy balance module

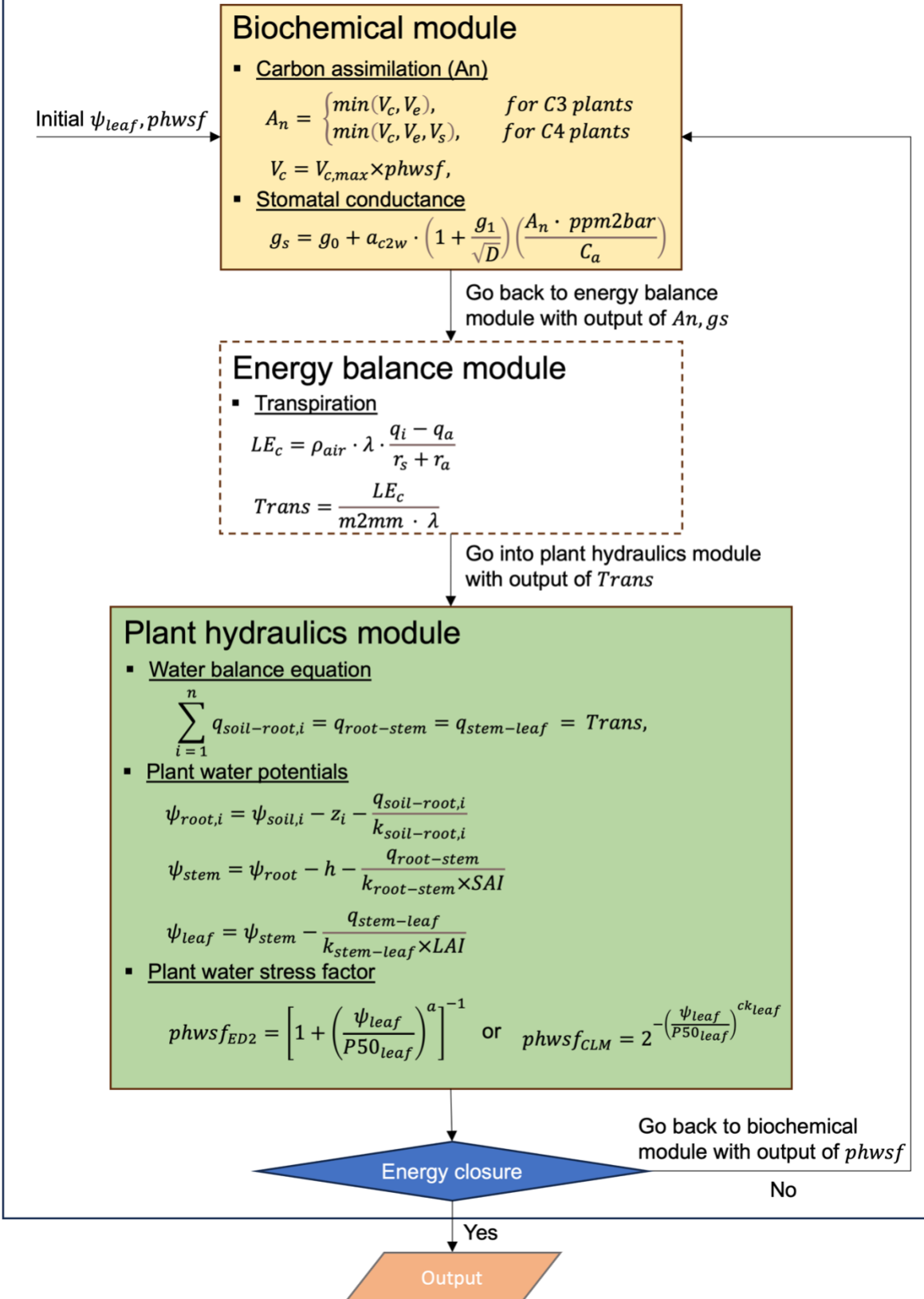


Fig. R12 Framework of the STEMMUS-SCOPE-PHS model.

Of the two formulae for plant water stress factor in Equations (8) and (9), which was used in the calculations shown in the subsequent figures and analyses?

Thank you for your comment. The $phwsf_{ED2}$ was used in the calculations shown in this research. We had revised the sentence as follows:

The plant water stress factor $phwsf_{ED2}$ is set as the default option in the STEMMUS-SCOPE-PHS, and is employed in this study.”

It is not explicit in the text or figure caption, but can we assume that the data are half-hourly values in Figures 5, 6 and 7?

We appreciate your comment. All the statistics displayed in Figures 5–7 in the main text are half-hourly results, and we have revised the manuscript accordingly (Fig. R5, Fig. R6, Fig. R13).

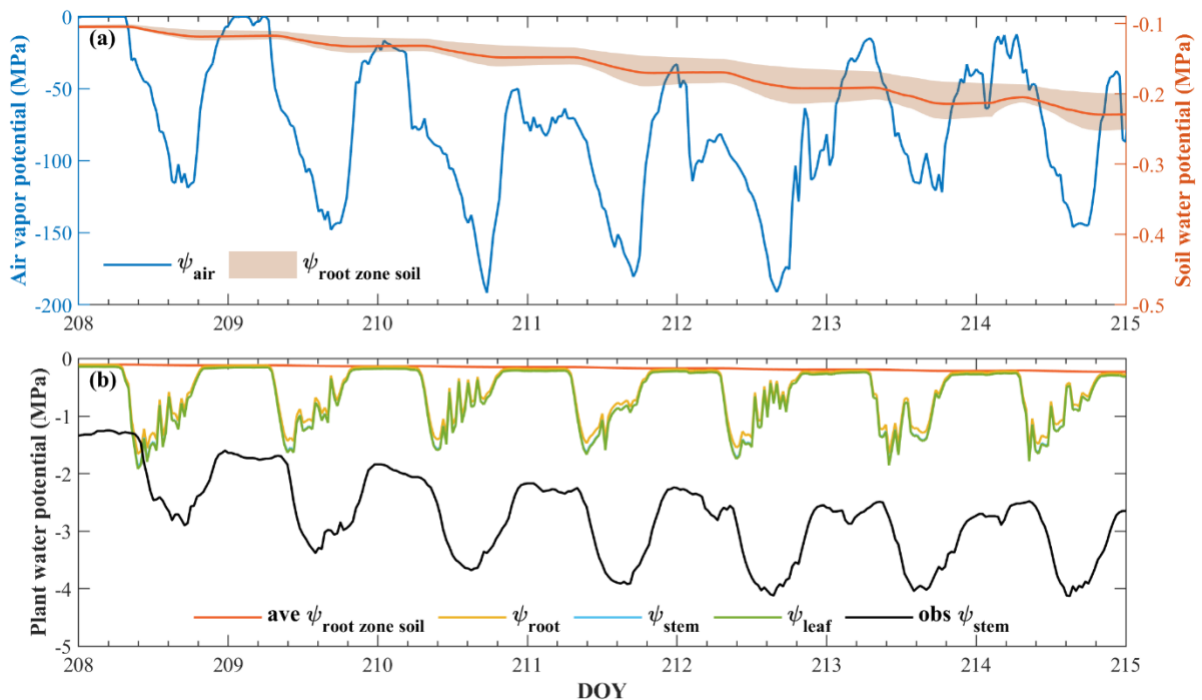


Fig. R13 Comparison of half-hourly simulated root zone soil ($\psi_{root\ zone\ soil}$), root (ψ_{root}), stem (ψ_{stem}), leaf (ψ_{leaf}) and air (ψ_{air}) water potential with observed stem water potential ($obs\ \psi_{stem}$).

In Figure 8 the statistics listed are identical between well-watered and water-limited conditions, so if the statistics are being estimated only on the window shown I find that unusual. If the stats should be different please change one set, but if they are estimated over the entire simulation period then one set can be removed.

Thank you for your comment. The statistics are calculated over the entire study period (i.e. from 1st January to 9th August, 2022) and are shown in Fig. R3 and Fig. R4. We have removed the statistics as shown in Figs.R5-8.

I agree with your conclusion that the assumption of constant internal water storage, as embodied in Equation (2), masks inertia in the system, internal redistribution, and limits the responsiveness of the formulation. It probably also limits any useful insights from the work.

Thank you for your comments. As shown in Fig. R5 and Fig. R6, the simulated half-hourly dynamics of latent heat fluxes (LE) and gross primary productivity (GPP) were improved by considering plant hydraulics pathway, and plant water stress factor.

In addition, the improvement of simulated latent heat fluxes indicated a more accurate energy distribution (Fig. R14). Specifically, the STEMMUS-SCOPE overestimated Bowen ratio during the daytime, which was improved by considering plant hydraulics process.

Our results indicate that the plant water storage is essential in diurnal dynamics of plant water stress. It will be included in STEMMUS-SCOPE model in the near future.

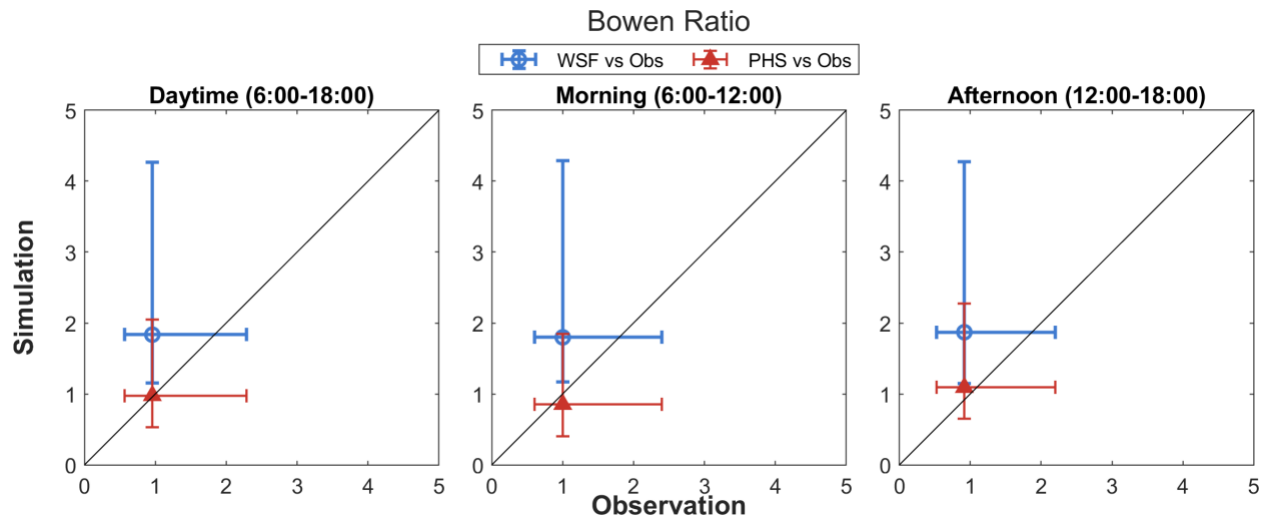


Fig. R14 Comparison of simulated Bowen ratio. The blue plot is the mean value of STEMMUS-SCOPE vs observation, and the red triangle is the mean value of STEMMUS-SCOPE-PHS vs observation. Daytime includes data from 6:00 to 18:00. Morning includes data from 6:00-12:00. Afternoon includes data from 12:00 to 18:00.

Bonan, G.B., 1993. Importance of leaf area index and forest type when estimating photosynthesis in boreal forests. *Remote Sensing of Environment*, 43(3): 303-314.

Fang, H., Wei, S. and Liang, S., 2012. Validation of MODIS and CYCLOPES LAI products using global field measurement data. *Remote Sensing of Environment*, 119: 43-54.

Tang, E. et al., 2024. Understanding the effects of revegetated shrubs on fluxes of energy, water, and gross primary productivity in a desert steppe ecosystem using the STEMMUS-SCOPE model. *Biogeosciences*, 21(4): 893-909.

van der Tol, C., Verhoef, W., Timmermans, J., Verhoef, A. and Su, Z., 2009. An integrated model of soil-canopy spectral radiances, photosynthesis, fluorescence, temperature and energy balance. *Biogeosciences*, 6(12): 3109-3129.

Wang, Y. et al., 2021. Integrated modeling of canopy photosynthesis, fluorescence, and the transfer of energy, mass, and momentum in the soil-plant-atmosphere continuum (STEMMUS-SCOPE v1.0.0). *Geoscientific Model Development*, 14(3): 1379-1407.